NUCL SCI TECH (2018) 29:181
https://doi.org/10.1007/s41365-018-0518-6

Light and heavy clusters in warm stellar matter

Helena Pais[1] · Francesca Gulminelli[2] · Constança Providência[1] · Gerd Röpke[3,4]

Received: 4 September 2018 / Revised: 8 November 2018 / Accepted: 8 November 2018 / Published online: 26 November 2018

Abstract Light and heavy clusters are calculated for warm stellar matter in the framework of relativistic mean-field models, in the single-nucleus approximation. The cluster abundances are determined from the minimization of the free energy. In-medium effects of light cluster properties are included by introducing an explicit binding energy shift analytically calculated in the Thomas–Fermi approximation, and the coupling constants are fixed by imposing that the virial limit at low density is recovered. The resulting light cluster abundances come out to be in reasonable agreement with constraints at higher density coming from heavy-ion collision data. Some comparisons with microscopic calculations are also shown.

Keywords Nuclear clusters · Warm stellar matter · In-medium effects

This work was partly supported by the FCT (Portugal) Project No. UID/FIS/04564/2016 and by former NewCompStar, COST Action MP1304. H.P. is supported by FCT (Portugal) under Project No. SFRH/BPD/95566/2013. She is very thankful to the Organizers of IWND 2018 for the opportunity to present this work, as well as the financial support received.

✉ Helena Pais
pais.lena@uc.pt

[1] CFisUC, Department of Physics, University of Coimbra, 3004-516 Coimbra, Portugal

[2] LPC (CNRS/ENSICAEN/Université de Caen Normandie), UMR6534, 14050 Caen Cédex, France

[3] Institut für Physik, Universität Rostock, 18051 Rostock, Germany

[4] National Research Nuclear University (MEPhI), Moscow, Russia 115409

1 Introduction

At densities below the nuclear saturation density and not too high temperatures ($T \lesssim 20$ MeV), core-collapse supernova matter is unstable with respect to density fluctuations such that inhomogeneous structures develop and clusters can appear. Light (deuterons, tritons, helions, α-particles) [1–6] and heavy (pasta phases) [7–14] nuclei can be expected. Besides core-collapse supernova matter [15], also neutron stars [16, 17] and neutron star mergers [18] are systems where light and heavy clusters may appear. These structures may have consequences in cooling of the object as they may change the neutrino mean free path [19–21].

This work follows the one in Ref. [22], where light clusters are calculated in the relativistic mean-field (RMF) framework [23]. Both in-medium mass shifts and in-medium modification of the cluster couplings are discussed. We also perform a new calculation for the heavy cluster within the compressible liquid drop (CLD) model, including light clusters. The results shown in this work will be further explored in a more detailed article, now in preparation [24].

At very low densities, we use the model-independent constraint, the virial EoS (VEoS) [1, 25, 26], to fix the cluster–meson couplings so that the VEoS particle fractions obtained in Ref. [26] are well reproduced. This constraint only depends on the experimentally determined binding energies and scattering phase shifts and provides the correct zero density limit for the equation of state at finite temperature.

In the high-density regime, the cluster dissolution mechanism is quite well described by the geometrical excluded volume mechanism [27, 28], so that we employ the Thomas–Fermi formulation of Ref. [29] to evaluate the associated cluster mass shift, and we obtain a simple

analytical formula for the effective mass shift. To reproduce empirical data, an in-medium modified coupling of cluster j with the scalar meson σ of the form $g_{sj} = x_s A_j g_s$ is proposed, where g_s is the coupling constant with the nucleons (n, p), A_j is the cluster mass number, and x_s is a universal cluster coupling fraction, with an associated uncertainty.

Besides the four standard charged light particles, ^{4}He, ^{3}H, ^{3}He, and ^{2}H, as the density increases, heavier clusters can also form, like ^{5}H, ^{7}H. Eventually, these clusters become very heavy, and the pasta phases appear. In this work, we are also interested in exploring the effect of such pasta structures within a CLD calculation [30] that includes light clusters with different sizes, since we want to understand if these heavier light clusters, which are usually ignored in pasta calculations, should also be included in calculations for stellar matter. The CLD calculation is based on the coexistence phase (CP) approximation, where the Gibbs equilibrium conditions are imposed to get the lowest free energy state, with the difference that in the CLD method, the surface and Coulomb terms are added to the free energy before the minimization is performed.

2 Theoretical description

We consider a system of protons and neutrons that interact via the exchange of mesons: the scalar σ, the vector ω, and the isovector ρ. Light clusters, deuteron (d), triton (t), helion (h), and α, are taken into account as new degrees of freedom. Electrons must also be included since we are dealing with stellar matter. The Lagrangian density, based on the nonlinear Walecka model, is given in Ref. [22].

The total binding energy of each cluster is defined as

$$B_j = A_j m^* - M_j^* , \tag{1}$$

with m^* the nucleon effective mass, and M_j^* the effective mass of each cluster, given by

$$M_j^* = A_j m - g_{sj}\phi_0 - \left(B_j^0 + \delta B_j\right), \tag{2}$$

where B_j^0 is the cluster binding energy in the vacuum, and δB_j is defined as [22]

$$\delta B_j = \frac{Z_j}{\rho_0}\left(\epsilon_p^* - m\rho_p^*\right) + \frac{N_j}{\rho_0}\left(\epsilon_n^* - m\rho_n^*\right). \tag{3}$$

The binding energy shift, δB_j, takes in-medium effects into account and needs to be determined. It is the energetic counterpart of the classical excluded volume mechanism. Since ϵ_j^* and ρ_j^* are the energy density and density of the gas in the lowest states, defined as

$$\epsilon_j^* = \frac{1}{\pi^2}\int_0^{p_{Fj}(\text{gas})} p^2 e_j(p)(f_{j+}(p) + f_{j-}(p))\mathrm{d}p , \tag{4}$$

$$\rho_j^* = \frac{1}{\pi^2}\int_0^{p_{Fj}(\text{gas})} p^2 (f_{j+}(p) + f_{j-}(p))\mathrm{d}p , \tag{5}$$

we avoid double counting because the energy states occupied by the gas are excluded. In the above expressions, $f_{j\pm}(p)$ are the Fermi distribution functions for the particles and anti-particles:

$$f_{j\pm}(p) = \frac{1}{\exp[(e_j(p) \mp v_j)/T] + 1}, \tag{6}$$

with $e_j(p) = \sqrt{p_j^2 + m^{*2}}$, and $v_j = \mu_j - g_v V_0 - g_\rho \tau_j b_0/2$, $j = n, p$.

The other quantity that considers in-medium effects is the scalar cluster–meson coupling, $g_{sj} = x_{sj} A_j g_s$, which is determined from experimental constraints. We fix x_{sj} so that in the low-density limit the virial EoS is reproduced. We obtained [22] $x_{sj} = 0.85 \pm 0.05$ as good universal scalar cluster–meson coupling that not only reproduces reasonably well the virial EoS but also reproduces well data coming from heavy-ion collisions in the high-density limit.

In the compressible liquid drop model (CLD) [30], matter is divided in two main regions: a high-density phase (I), where the heavy cluster forms, and the low-density phase (II), where a background nucleon gas exists and where the light clusters can form.

We obtain the equilibrium conditions of the system from the minimization of the total free energy, including the surface and Coulomb terms. The free energy density is given by

$$F = fF^I + (1-f)F^{II} + F_\mathrm{e} + \varepsilon_\text{surf} + \varepsilon_\text{Coul}. \tag{7}$$

This minimization is done with respect to four variables: the size of the geometric configuration, r_d, which gives, just like in the CP case, the condition $\varepsilon_\text{surf} = 2\varepsilon_\text{Coul}$, the baryonic density in the high-density phase, ρ^I, the proton density in the high-density phase, ρ_p^I, and the volume fraction of the high-density phase, f, defined as

$$f = \frac{\rho - \rho^{II}}{\rho^I - \rho^{II}} . \tag{8}$$

The equilibrium conditions then become

$$\begin{aligned} P^I &= P^{II} - \varepsilon_\text{surf}\left(\frac{1}{2\alpha} + \frac{1}{2\Phi}\frac{\partial\Phi}{\partial f} - \frac{\rho_p^{II}}{f(1-f)(\rho_p^I - \rho_p^{II})}\right), \\ \mu_n^I &= \mu_n^{II} , \\ \mu_p^I &= \mu_p^{II} - \frac{\varepsilon_\text{surf}}{f(1-f)(\rho_p^I - \rho_p^{II})} , \end{aligned} \tag{9}$$

with $\alpha = f$ for droplets, rods, and slabs, $\alpha = 1 - f$ for tubes and bubbles. The expression for Φ depends on the dimension, D, and volume fraction, f, of the heavy clusters, and is given by Ref. [30]

$$\Phi = \begin{cases} \left(\frac{2 - D\alpha^{1-2/D}}{D-2} + \alpha\right)\frac{1}{D+2}, & D = 1, 3 \\ \frac{\alpha - 1 - \ln\alpha}{D+2}, & D = 2. \end{cases} \quad (10)$$

For each phase, the light clusters, which we extend to $A = 12$, are in chemical equilibrium, with the chemical potential of each cluster defined as:

$$\begin{aligned} \mu^I_{Acl} &= N\mu^I_n - Z\mu^I_p, \\ \mu^{II}_{Acl} &= N\mu^{II}_n - Z\mu^{II}_p, 2 \le A_{\rm cl} \le 12, \end{aligned} \quad (11)$$

and charge neutrality must also be imposed:

$$\rho_{\rm e} = Y_p\rho = f\rho^I_{\rm c} + (1-f)\rho^{II}_{\rm c}, \quad (12)$$

with $\rho_{\rm e}$ the electron density and $\rho_{\rm c}$ the charge density. Equations (9), (11), and (12) need to be solved self-consistently for the low-energy state to be found.

3 Results and discussion

In the following, we show some of the results obtained in this work, at finite fixed temperatures and for fixed proton fractions y_p which describes the ratio of the total proton density to the baryon density. We start by explaining how we determined the cluster–meson coupling fraction, x_s, from the virial equation of state (VEoS). Then we investigate the effect of introducing the binding energy shift δB_j, and its consequence on the clusters distributions, and we also calculate the equilibrium constants, comparing our results with data coming from heavy-ion collisions [31]. Finally, a calculation with heavy cluster from a compressible liquid drop (CLD) approximation is done, where we also include light clusters with a nucleon number, A, up to 12.

3.1 Determination of x_s: Virial EoS

The cluster–meson couplings are obtained from the best fit of the RMF cluster mass fractions, defined as $X_j = A_j n_j/n$, to the VEoS data, taking the FSU parametrization [32] model. This model has been chosen because it describes adequately the properties of nuclear matter at saturation and subsaturation densities. The fit is done choosing a sufficiently low density close to the cluster onset, where the virial EoS is still valid, and, at the same time, the interaction already has non-negligible effects. We have considered densities between 10^{-6}fm^{-3} and 10^{-4}fm^{-3}, a range of densities where we expect the VEoS to be a good approximation. In this low-density domain, the binding energy shift δB_j of Eq. (3) is completely negligible and does not affect the particle fractions (see also Fig. 2); therefore, it was put to zero for this calculation.

Only the g_{sj} parameters are optimized,

$$g_{sj} = x_{sj}A_j g_s, \quad (13)$$

while the vector couplings are set to

$$g_{vj} = A_j g_v. \quad (14)$$

Reasonable values for g_{sj} are $(0.85 \pm 0.05)A_j g_s$, see Fig. 1, where the colored bands show the range of particle fractions covered by this interval at low densities, for T =4 and 10 MeV. The solid vertical black lines, defined by $\rho\lambda_n^3 = 1/10$ [26], ρ being the baryon density and λ_n the nucleon thermal wavelength, represent the upper limit of the region of validity of the VEoS. Looking at this figure,

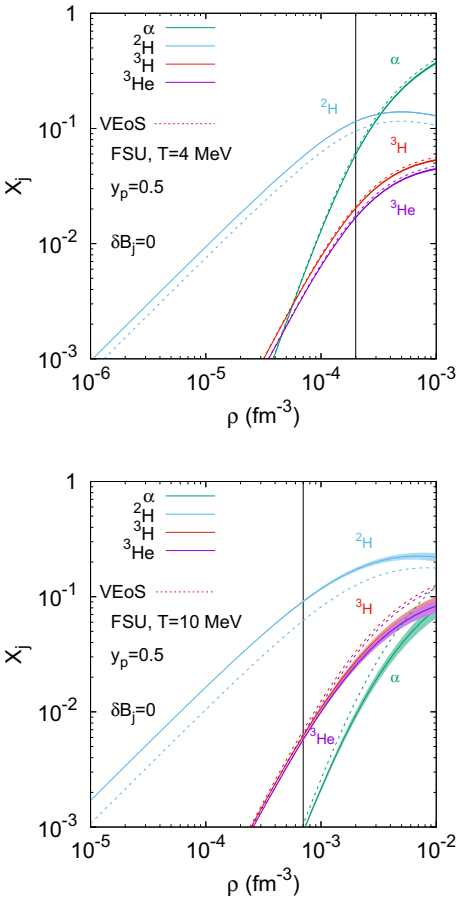

Fig. 1 (Color online) Fraction of deuteron, X_d, triton, X_t, helion, X_h, and α, X_α, as a function of the density for FSU, $T = 4$ MeV (top) and 10 MeV (bottom), with proton fraction $y_p = 0.5$, taking $\delta B = 0$, $x_{sj} = 0.85 \pm 0.05$, (variation indicated by the spreading of the bands), and comparing with results of the virial EoS from [26]. Solid vertical black lines are given by $\rho\lambda_n^3 = 1/10$

we see that the only cluster fraction that is not consistent with the VEoS result is the deuteron. This can be explained by the fact that this cluster is the less bound cluster we are considering, and mean-field models usually fail to describe such systems. This is an effect of the continuum contribution of the deuteron channel, as was pointed out in Ref. [33]: its contribution is essential if the binding energy per nucleon is small when compared with T.

3.2 Effect of the binding energy shift δB_j

Let us now discuss the effect of introducing a nonzero binding energy shift δB_j, Eq. (3). In Fig. 2, we compare the binding energy of the α-clusters, obtained taking δB_α, as defined by Eq. (3), with the binding energy

$$B_j = B_j^0 + \delta B_j^{\rm QS} \tag{15}$$

obtained from quantum statistical (QS) calculations, with $\delta B_j^{\rm QS}(P;\rho_n,\rho_p,T)$ taking different center-of-mass momenta $P = 0, 1, 2$ fm^{-1}, according to Ref. [33].

Also shown in this figure is a QS calculation from a perturbative approach where the Pauli blocking shift of α particles with center-of-mass momentum (wave number) $P = 0$ was obtained at the lowest order of density ρ [34]

$$\delta B_\alpha^{\rm Pauli}(P=0;\rho_n,\rho_p,T) = -\frac{164371\ \rho}{(T+10.67)^{3/2}} \tag{16}$$

(in units of MeV, with T in units of MeV, and ρ in units of fm^{-3}). Lastly, Fig. 2 also shows a calculation from Typel et al. [35], where, in order to suppress cluster formation at higher densities, they introduced an empirical quadratic form given by

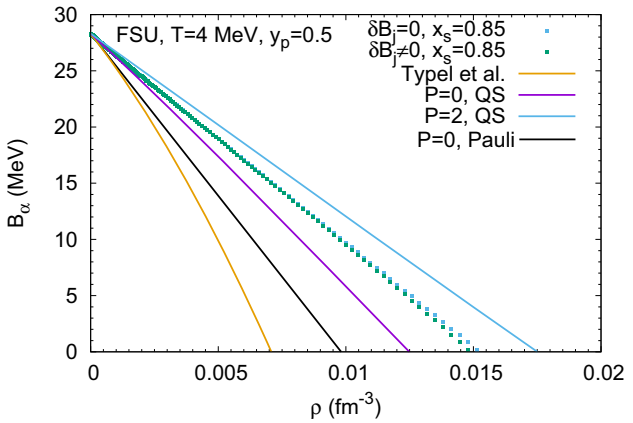

Fig. 2 (Color online) Binding energy of α for the RMF-FSU calculation (this work), $T = 4$ MeV, and $y_p = 0.5$ obtained with Eq. (2). For comparison, results neglecting the binding energy shift (3) ($\delta B_j = 0$), as well as the empirical form Eq. (17) from Typel et al. [35], and results obtained from a recent QS approach [33] for different center-of-mass momenta, P (in units of fm^{-1}), and a QS calculation of a perturbative approach [34] (Pauli), Eq. (16), are also shown

$$\delta B_\alpha^{\rm Typel}(T) = \delta B_\alpha^{\rm Pauli}(P=0;\rho_n,\rho_p,T) \times \left[1 - \frac{\delta B_\alpha^{\rm Pauli}(P=0;\rho_n,\rho_p,T)}{2B_\alpha^0}\right]. \tag{17}$$

We can see from Fig. 2 that the additional binding energy shift δB_j given by Eq. (3) is completely negligible in the domain of validity of the VEoS, which means that the cluster couplings do not depend on this term. Even for higher densities and still in the range where the total binding energy of the clusters is positive, this extra correction is small but will rise fast as the density increases, as it can be seen in the next figure.

It is also interesting to discuss the effect of the coupling x_{sj} and temperature T on the binding energy shift. From Fig. 3 we conclude that the larger x_{sj} the slower $-\delta B_j$ increases and also that a larger temperature determines a softer behavior, with $-\delta B_j$ taking larger values at the lower densities and smaller ones close to the dissolution density.

However, we should stress that Figs. 2 and 3 do not give a complete picture of the in-medium effects and cluster dissolution mechanism, because the mass shift strongly modifies the equations of motion for the meson fields. The particle fractions are thus affected in a highly complex way because of the self-consistency of the approach, which additionally induces temperature effects, as we will see next.

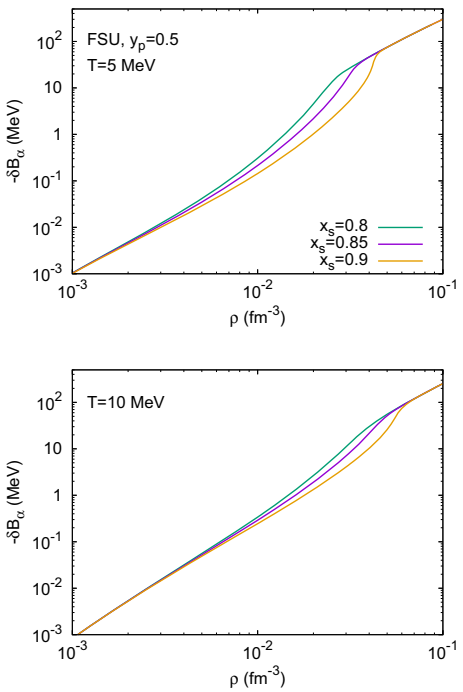

Fig. 3 (Color online) Binding energy shift of α, δB_α, as given by Eq.(3) for the RMF-FSU calculation, $y_p = 0.5$, $T = 5$ MeV (top), and $T = 10$ MeV (bottom), for $x_s = 0.8, 0.85, 0.9$

3.3 Effect of δB_j on the global cluster distributions

We show in the present subsection that the clusters are dissolved below the nuclear saturation density, ρ_0. In Fig. 4, we show the clusters mass fractions for matter with a fixed proton fraction of $y_p = 0.41$, $T = 5$ MeV, and $x_{sj} = 0.85$. We observe that if we neglect the δB_j term, the clusters do not dissolve, which is precisely the role of this extra term in the binding energy. For the temperatures and proton fractions presented, the typical values for the dissolution ($X_j < 10^{-4}$) of light clusters are within the density range $0.04\,\mathrm{fm}^{-3} < \rho < 0.06\,\mathrm{fm}^{-3}$.

3.4 Equilibrium constants

In the high-density limit, a constraint was proposed in Ref. [31]. These chemical equilibrium constants, $K_c[j]$, calculated with data from heavy-ion collisions, are defined as

$$K_c[j] = \frac{\rho_j}{\rho_n^{N_j}\,\rho_p^{Z_j}}, \tag{18}$$

where ρ_j is the number density of cluster j, with neutron number N_j and proton number Z_j, and ρ_p, ρ_n are, respectively, the number densities of free protons and neutrons. For this calculation we fix the proton fraction to 0.41 as was done in [31, 36].

In Fig. 5, we show the chemical equilibrium constants for all the light clusters considered, taking the range of the couplings to be $g_{sj} = (0.85 \pm 0.05)\,A_j g_s$, and we compare with the experimental results of Ref. [31]. We can see that taking the coupling fractions $x_{sj} = 0.85 \pm 0.05$ essentially describes the experimental equilibrium constants. We have checked that $x_s = 0.95$ would be too large.

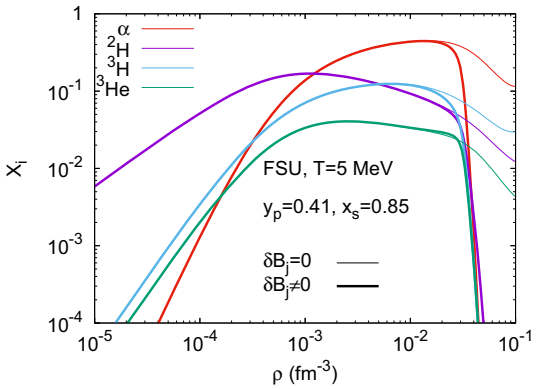

Fig. 4 (Color online) Fraction of α, X_α (red), deuteron, X_d (violet), triton, X_t (light blue), and helion, X_h (green), as a function of the density for FSU, $T = 5$ MeV, and $y_p = 0.41$, with (thick) and without (thin) δB_j, for $x_{sj} = 0.85$, keeping δB_j

These experimental data seem to put extra constraints, that together with VEoS, suggest that a good universal coupling for all clusters is $g_{sj} = (0.85 \pm 0.05)\,A_j\,g_s$. For the deuteron, the experimental data seem to be described by the upper limit $x_s = 0.9$. Possibly a more detailed approach would allow for a different coupling g_{sj} for each cluster.

3.5 Influence on the pasta structure

Until now, we have considered homogeneous matter (HM) with light clusters. We next test how is the fraction of heavy clusters (pasta) affected with the inclusion of the light clusters. For that, we consider a CLD calculation with light clusters, where the inclusion of the binding energy shift term of the light clusters, δB_j, is also considered. The heavy cluster is always calculated in the droplet configuration.

Another important remark is that, besides considering the 4 usual light clusters, i.e., ^{4}He, ^{2}H, ^{3}H, and ^{3}He, we are also taking all the bound clusters with $A \leq 12$.

In Fig. 6, we show for a fixed proton fraction of 0.2 and $T = 5, 7$ MeV, the total mass fraction of clusters, light and heavy, in both a CLD and a HM calculation. For the cluster–meson couplings, we are taking $x_s = 0.85$, and, in all calculations, $x_v = 1$, with $g_{s_i} = x_s g_s A_i$ and $g_{v_i} = x_v g_v A_i$. Looking at the abundance of light clusters, we see that it is higher in the HM calculation, because the CLD also considers the heavy cluster. However, the melting of these clusters in the CLD case occurs at a higher density. If we consider the heavy cluster abundancy, we see that it decreases when the calculation includes light clusters, and its onset occurs at a higher density as compared to the CLD case. The background of free nucleons is also higher in this case.

4 Summary

In summary, a simple parametrization of in-medium effects acting on light clusters was proposed in a RMF framework. The interactions of the clusters with the medium were described by a modification of the σ-meson coupling constant. The cluster dissolution was obtained by the density-dependent extra term on the binding energy, δB_j. The fraction $x_{sj} = 0.85 \pm 0.05$ reproduces both virial limit and K_c from HIC. The inclusion in the CLD (heavy cluster) calculation of a larger number of degrees of freedom through light clusters not only reduces the size of the heavy cluster but also increases the fraction of free nucleons in the background gas. Overall, we find that the influence of light, loosely bound clusters, beside ^{2}H, ^{3}H, ^{3}He, and ^{4}He, is not negligible, and they should be

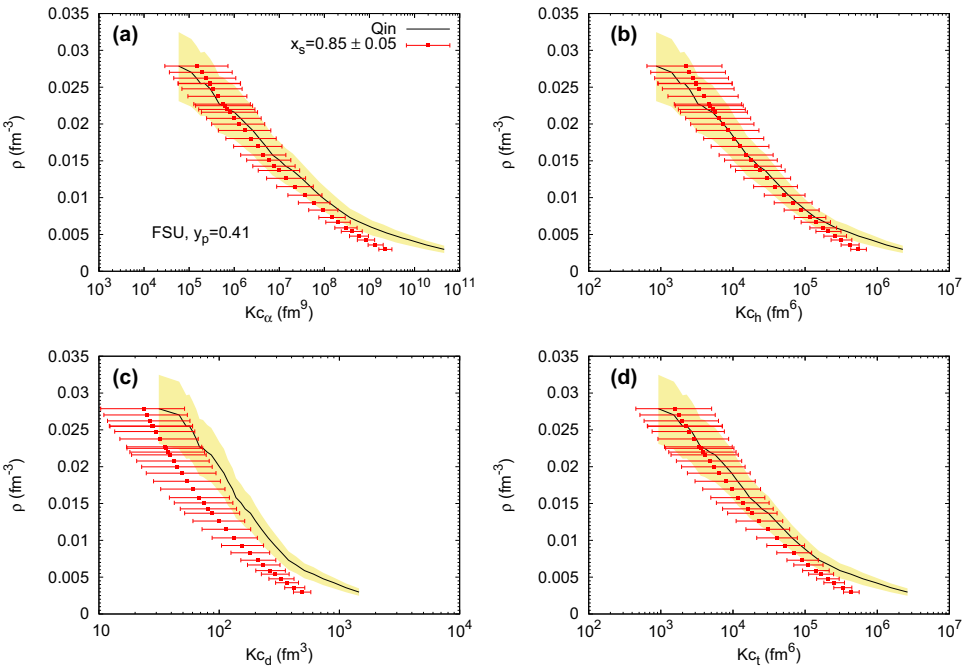

Fig. 5 (Color online) Chemical equilibrium constants of α (a), helion (b), deuteron (c), and triton (d) for FSU, and $y_p = 0.41$, and the universal g_{sj} fitting with $g_{sj} = (0.85 \pm 0.05)\, A_j\, g_s$, (red dotted lines). The experimental results of Qin et al [31] (yellow region) are also shown

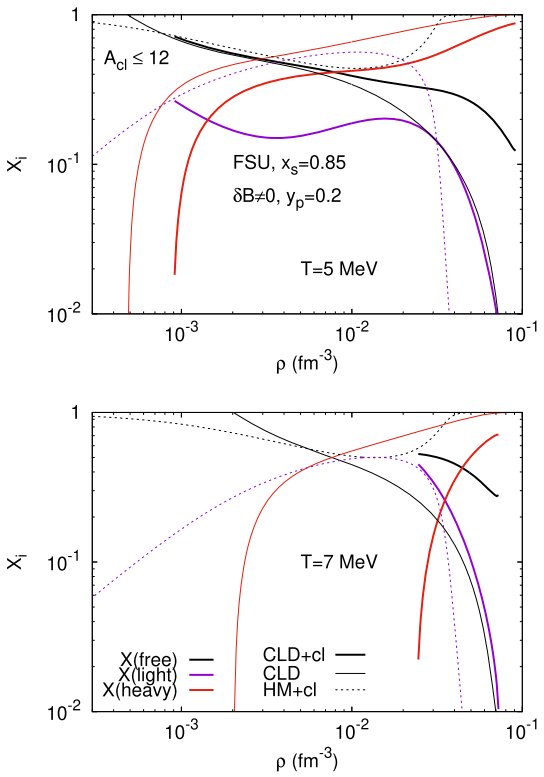

Fig. 6 (Color online) Total mass fraction of free particles (black), and light clusters (violet), for a CLD with (thick) and without (thin) light clusters, and HM (dashed) calculations for FSU, $y_p = 0.2$, and $x_s = 0.85, x_v = 1$, with $T = 5$ MeV (top) and $T = 7$ MeV (bottom). The heavy cluster mass fraction (red) from a CLD calculation is also shown. All the results shown take $\delta B_j \neq 0$. In both calculations we are taking A_{cl} up to 12

explicitly included in the EoS for core-collapse supernova simulations and neutron star mergers.

References

1. C.J. Horowitz, A. Schwenk, Cluster formation and the virial equation of state of low-density nuclear matter. Nucl. Phys. A **776**, 55–79 (2006). https://doi.org/10.1016/j.nuclphysa.2006.05.009
2. S. Typel, G. Röpke, T. Klähn et al., Composition and thermodynamics of nuclear matter with light clusters. Phys. Rev. C **81**, 015803 (2010). https://doi.org/10.1103/PhysRevC.81.015803
3. S.S. Avancini, C.C. Barros Jr., L. Brito et al., Light clusters in nuclear matter and the "pasta" phase. Phys. Rev. C **85**, 035806 (2012). https://doi.org/10.1103/PhysRevC.85.035806
4. A. Raduta, F. Gulminelli, Statistical description of complex nuclear phases in supernovae and proto-neutron stars. Phys. Rev. C **82**, 065801 (2010). https://doi.org/10.1103/PhysRevC.82.065801
5. M. Hempel, J. Schaffner-Bielich, A statistical model for a complete supernova equation of state. Nucl. Phys. A **837**, 210–254 (2010). https://doi.org/10.1016/j.nuclphysa.2010.02.010
6. M. Ferreira, C. Providência, Description of light clusters in relativistic nuclear models. Phys. Rev. C **85**, 055811 (2012). https://doi.org/10.1103/PhysRevC.85.055811
7. D.G. Ravenhall, C.J. Pethick, J.R. Wilson, Structure of matter below nuclear saturation density. Phys. Rev. Lett. **50**, 2066 (1983). https://doi.org/10.1103/PhysRevLett.50.2066
8. C.J. Horowitz, M.A. Pérez-García, D.K. Berry et al., Dynamical response of the nuclear "pasta" in neutron star crusts. Phys. Rev. C **72**, 035801 (2005). https://doi.org/10.1103/PhysRevC.72.035801
9. T. Maruyama, T. Tatsumi, D. Voskresensky et al., Nuclear "pasta" structures and the charge screening effect. Phys. Rev. C **72**, 015802 (2005). https://doi.org/10.1103/PhysRevC.72.015802

10. G. Watanabe, T. Maruyama, K. Sato et al., Simulation of transitions between "Pasta" phases in dense matter. Phys. Rev. Lett. **94**, 031101 (2005). https://doi.org/10.1103/PhysRevLett.94.031101
11. H. Sonoda, G. Watanabe, K. Sato, et al., Erratum: Phase diagram of nuclear "pasta" and its uncertainties in supernova cores [Phys. Rev. C 77, 035806 (2008)]. Phys. Rev. C **81**, 049902 (2010). https://doi.org/10.1103/PhysRevC.81.049902
12. H. Pais, J.R. Stone, Exploring the nuclear pasta phase in core-collapse supernova matter. Phys. Rev. Lett. **109**, 151101 (2012). https://doi.org/10.1103/PhysRevLett.109.151101
13. A.S. Schneider, D.K. Berry, C.M. Briggs et al., Nuclear "waffles". Phys. Rev. C **90**, 055805 (2014). https://doi.org/10.1103/PhysRevC.90.055805
14. F. Grill, H. Pais, C. Providência et al., Equation of state and thickness of the inner crust of neutron stars. Phys. Rev. C **90**, 045803 (2014). https://doi.org/10.1103/PhysRevC.90.045803
15. M. Oertel, M. Hempel, T. Klähn et al., Equations of state for supernovae and compact stars. Rev. Mod. Phys. **89**, 015007 (2017). https://doi.org/10.1103/RevModPhys.89.015007
16. N.K. Glendenning, in *Compact Stars: Nuclear Physics, Particle Physics, and General Relativity*, ed. by N.K. Glendenning (Springer, New York, 2000)
17. P. Haensel, A. Y. Potekhin, D. G. Yakovlev, in *Neutron Stars 1: Equation of State and Structure*, ed. by P. Haensel, A.Y. Potekhin, D.G. Yakovlev (Springer, New York, 2007)
18. B.P. Abbott et al., LIGO and Virgo Collab., GW170814: a three-detector observation of gravitational waves from a binary black hole coalescence. Phys. Rev. Lett **119**, 141101 (2017). https://doi.org/10.1103/PhysRevLett.119.141101
19. A. Arcones, G. Martínez-Pinedo, E. O'Connor et al., Influence of light nuclei on neutrino-driven supernova outflows. Phys. Rev. C **78**, 015806 (2008). https://doi.org/10.1103/PhysRevC.78.015806
20. S. Furusawa, H. Nagakura, K. Sumiyoshi et al., The influence of inelastic neutrino reactions with light nuclei on the standing accretion shock instability in core-collapse supernovae. Astrophys. J. **774**, 78 (2013). https://doi.org/10.1088/0004-637X/774/1/78
21. S. Furusawa, K. Sumiyoshi, S. Yamada et al., Supernova equations of state including full nuclear ensemble with in-medium effects. Nucl. Phys. A **957**, 188–207 (2017). https://doi.org/10.1016/j.nuclphysa.2016.09.002
22. H. Pais, F. Gulminelli, C. Providência et al., Light clusters in warm stellar matter: explicit mass shifts and universal cluster-meson couplings. Phys. Rev. C **97**, 045805 (2018). https://doi.org/10.1103/PhysRevC.97.045805
23. M. Dutra, O. Lourenço, S.S. Avancini et al., Relativistic mean-field hadronic models under nuclear matter constraints. Phys. Rev. C **90**, 055203 (2014). https://doi.org/10.1103/PhysRevC.90.055203
24. H. Pais, F. Gulminelli, C. Providência, G. Röpke (in preparation)
25. C.J. Horowitz, A. Schwenk, The virial equation of state of low-density neutron matter. Phys. Lett. B **638**, 153–159 (2006). https://doi.org/10.1016/j.physletb.2006.05.055
26. M.D. Voskresenskaya, S. Typel, Constraining mean-field models of the nuclear matter equation of state at low densities. Nucl. Phys. A **887**, 42–76 (2012). https://doi.org/10.1016/j.nuclphysa.2012.05.006
27. M. Hempel, J. Schaffner-Bielich, S. Typel et al., Light clusters in nuclear matter: excluded volume versus quantum many-body approaches. Phys. Rev. C **84**, 055804 (2011). https://doi.org/10.1103/PhysRevC.84.055804
28. H. Pais, S. Typel, in *Comparison of Equation of State Models with Different Cluster Dissolution Mechanisms in Nuclear Particle Correlations and Cluster Physics*, ed. by W.U. Schröder (Schröder, World Scientific, 2017). arXiv:1612.07022
29. F. Gulminelli, AdR Raduta, Unified treatment of subsaturation stellar matter at zero and finite temperature. Phys. Rev. C **92**, 055803 (2015). https://doi.org/10.1103/PhysRevC.92.055803
30. H. Pais, S. Chiacchiera, C. Providência, Light clusters, pasta phases, and phase transitions in core-collapse supernova matter. Phys. Rev. C **91**, 055801 (2015). https://doi.org/10.1103/PhysRevC.91.055801
31. L. Qin, K. Hagel, R. Wada et al., Laboratory tests of low density astrophysical nuclear equations of state. Phys. Rev. Lett. **108**, 172701 (2012). https://doi.org/10.1103/PhysRevLett.108.172701
32. B.G. Todd-Rutel, J. Piekarewicz, Neutron-rich nuclei and neutron stars: a new accurately calibrated interaction for the study of neutron-rich matter. Phys. Rev. Lett. **95**, 122501 (2005). https://doi.org/10.1103/PhysRevLett.95.122501
33. G. Röpke, Nuclear matter equation of state including two-, three-, and four-nucleon correlations. Phys. Rev. C **92**, 054001 (2015). https://doi.org/10.1103/PhysRevC.92.054001
34. G. Röpke, Light nuclei quasiparticle energy shifts in hot and dense nuclear matter. Phys. Rev. C **79**, 014002 (2009). https://doi.org/10.1103/PhysRevC.79.014002
35. S. Typel, G. Röpke, T. Klähn et al., Composition and thermodynamics of nuclear matter with light clusters. Phys. Rev. C **81**, 015803 (2010). https://doi.org/10.1103/PhysRevC.81.015803
36. M. Hempel, K. Hagel, J. Natowitz et al., Constraining supernova equations of state with equilibrium constants from heavy-ion collisions. Phys. Rev. C **91**, 045805 (2015). https://doi.org/10.1103/PhysRevC.91.045805